sustainability

Article

Settlement Analysis of Ground Surface and Adjacent Building Caused by Driving and Expansion Excavation of Shield Tunnel Using Artificial Freezing Method

Xiaoming Guan [1], Ruohui Wang [1], Hongxian Fu [2,3,*], Wei Feng [4], Xin Jin [1], Shuqin Li [5], Shaohui Xu [1] and Jiguang Li [6]

[1] School of Civil Engineering, Qingdao University of Technology, Qingdao 266520, China; guanxiaoming@qut.edu.cn (X.G.); wang_rhui@163.com (R.W.); jx1051994273@163.com (X.J.); xush7321@163.com (S.X.)
[2] Key Laboratory of Urban Underground Engineering of Ministry of Education, Beijing Jiaotong University, Beijing 100044, China
[3] School of Civil Engineering, Beijing Jiaotong University, Beijing 100044, China
[4] Shandong Hi-Speed Engineering Construction Group Co., Ltd., Jinan 250014, China; arch_w@126.com
[5] Shandong Sanjian Construction Projects Stock Co., Ltd., Jinan 250100, China
[6] The NO.2 Engineering Company of China Railway 20nd Bureau Group Co., Ltd., Beijing 100013, China; yyyk202@163.com
* Correspondence: fhxllj@163.com

Abstract: The artificial freezing method can effectively improve the stability of strata and provide favorable conditions for the construction safety of shield tunnel in water-rich strata. Based on the frozen shield tunneling project of a metro station, which is close to important buildings, a reasonable freezing method and parameters are proposed in this paper. The simulation model was established by using Plaxis 3D finite element software (Version 2017). The numerical model was verified based on a large amount of field data. The characteristics of segment deformation, ground surface settlement and vertical displacement of buildings were compared between frozen layer and nonfrozen layer during shield tunnel excavation. It was found that segment deformation in the nonfrozen layer is three times that in the frozen layer. The surface settlement above the frozen layer is less than 2 mm. Expansion excavation of shield tunnel was carried out to meet the space function of subway station using artificial freezing method. The deformation of frozen layer was compared between full section excavation and partial excavation. It was found that the deformation of the former is 4.5 times that of the latter, so the partial excavation was chosen as the main research object. Subsequently, the characteristics of vertical displacement and surface settlement of buildings under partial excavation were studied. It was found that the vertical settlement of buildings away from the frozen layer is greater than that of buildings near the frozen layer. All settlement values meet the requirements, thus ensuring the feasibility of partial excavation and ensuring the safety of construction.

Keywords: shield tunnel; artificial freezing method; expansion excavation; settlement analysis; building

Citation: Guan, X.; Wang, R.; Fu, H.; Feng, W.; Jin, X.; Li, S.; Xu, S.; Li, J. Settlement Analysis of Ground Surface and Adjacent Building Caused by Driving and Expansion Excavation of Shield Tunnel Using Artificial Freezing Method. *Sustainability* **2023**, *15*, 14166. https://doi.org/10.3390/su151914166

Academic Editors: Pengjiao Jia, Peixin Shi, Cheng Cheng and Xi Jiang

Received: 1 September 2023
Revised: 22 September 2023
Accepted: 23 September 2023
Published: 25 September 2023

1. Introduction

The artificial freezing method (AFM) originated from mine construction. In recent years, with the development of China's economy and the increase in urban construction, the AFM has gradually expanded its application field and thus become the main construction method of municipal metro construction [1–3]. The AFM is widely used in water-rich strata. The AFM can effectively improve the stability of strata and provide favorable conditions for tunnel construction [4,5]. Zhou proposed a more accurate actual frost heave prediction method based on multilayer field tests and segregation potential model, aiming at an AFM project with strict deformation requirements during normal airport operations.

This method provides a valuable reference for the normal operation of airports or tunnel construction near existing buildings [6]. Liu, Zhang, Russo and Cai et al. studied the freezing construction of the GangBei tunnel of the Hong Kong–Zhuhai–Macao bridge using the pipe jacking method and proposed a theoretical model of formation displacement prediction. They found the factors affecting the strata displacement, analyzed the surface settlement, and solved the technical problems of ultra-shallow buried large section tunnels passing under sensitive buildings under complex geological conditions [7–9]. Ding proposed that surface settlement presents cork distribution curve characters, skewed distribution curve characteristics, and normal distribution curve characteristics when the tunnel is, respectively, under buildings, within the scope of the disturbance, and outside the scope of the disturbance. The research findings can be used to make effective prediction of ground surface settlement caused by tunnel construction of adjacent buildings [10]. Zheng combined laboratory experiments and numerical simulations to propose a method that can be used to simulate and predict surface deformation during the entire construction process of the AFM [11]. Xiang took the tunnel from Yixian Bridge to Daxinggong section of Nanjing Metro Line 2 as the research object. Based on the discrete element thermal–force coupling theory, the numerical modeling of horizontal freezing reinforcement engineering was established, which provides a feasible method for predicting surface displacement [12]. Ren studied the temperature field of the freezing process of the new curtain by means of numerical simulation and found the mechanism of the active freezing and thawing process of the new curtain freezing method in construction [13].

In urban metro construction, the shield is usually used to excavate the tunnel [14], and the cut and cover method or shallow tunnelling method is usually used in subway stations [15,16]. In the case that the traditional construction method cannot be implemented, the scheme of metro station expansion on the basis of a large-diameter shield tunnel is put forward. Wang proposed for the first time the shield passing through the air passage mode of “shield passing first and then constructing the air passage structure”. It breaks through the conventional mode of “forming the air tunnel structure first, and then the shield passes through”. The contradiction between tunnel construction and station construction was solved successfully. The method of using large-diameter shield tunnel as construction channel and working platform to expand the station was created [17]. Xu studied the metro station expansion of large-diameter shield tunnels using the pile–beam–arch and found the law of surface settlement during construction [18]. Liu studied the surface deformation characteristics caused by shield tunneling construction through a large amount of simulation data and field data. It was found that horizontal displacement and vertical displacement are two important factors leading to building deformation and cracks [19]. Li used the finite element method of “strata–structure” interaction to analyze the key conditions of metro station construction by expanding a large-diameter shield tunnel with the PBA construction method. The construction mechanism of the two sides of the shield tunnel asymmetric excavation and the two sides of the K-segment asymmetric removal of the key conditions was studied. The design schemes of the supporting parameters, excavation method, and removal method of K-segment were optimized [20,21]. Lv analyzed the influence rules of shield tunneling on ground subsidence under the condition of different hard rock height ratios. In the process of crossing different hard rock height ratio composite strata, as the hard rock height ratio decreases, the value of ground settlement decreases and the settlement tank becomes shallow [22].

At present, research on the artificial freezing method in subway construction mainly focuses on the prediction of surface settlement and the research of freezing parameters. It mainly relies on numerical simulation and theoretical analysis. The expansion of shield tunnel in a water-rich sand layer has not been studied. This paper combines a large amount of field data and numerical simulation methods. Based on a metro station project, a cup-type freezing method for shield tunnels is proposed, which is suitable for water-rich sand clay strata. In the process of shield excavation, the regularity of segment deformation, building vertical displacement, and surface settlement caused by frozen layers and nonfrozen layers are compared and analyzed. Based on the frozen expansion engineering of shield tunnels in water-rich sand strata, the deformation of frozen layers, vertical displacement of buildings, and surface settlement caused by different excavation methods are compared and analyzed. Finally, the optimized excavation construction method is proposed, which can effectively be used control formation/deformation and ensure the safety of excavation construction.

2. Project Overview

2.1. Project Overview and Freezing Parameters

A subway station in Zhengzhou is an underground three-level island platform station, as shown in Figure 1. The length of the main body of the station is about 163.25 m, and the depth of the standard section is about 26.85 m. The main body of the station was constructed using the cut and cover method, and the main structure of the station is a reinforced concrete box structure. Both ends of the station are subway shield sections, and both ends are shield starting points. The design mileage of the right line is 671.195 m, and the design mileage of the left line is 659.946 m. An earth pressure balancing shield machine is used for both left and right line shield tunneling, it is frozen starting, and the tunnel burial depth of the starting section is about 24.94 m. The protective structure of the shield tunnel at the station is a 1000 mm thick underground diaphragm wall. The shield segments are made of C50 reinforced concrete with an outer diameter of 6.2 m and an inner diameter of 5.5 m.

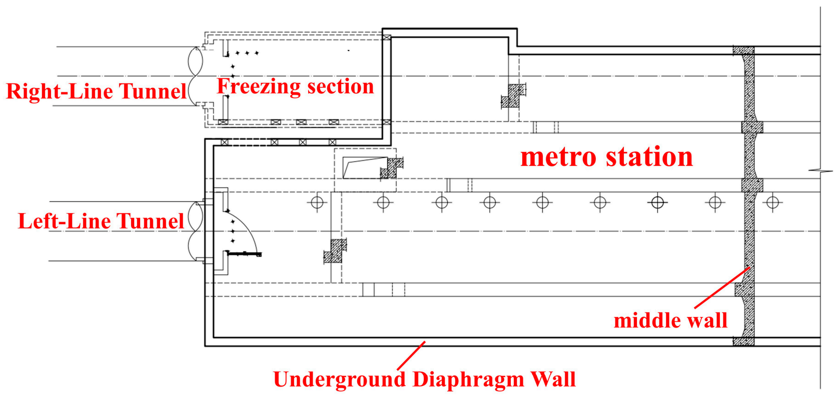

Figure 1. Metro station plan.

The main reason for the expansion of the tunnel was to consider the increase in ridership, and the subway was originally designed to use B-type cars, but now uses A-type cars. The bored tunnel is 18 m in total, the height of the vault from the ground is 16.31 m, and the whole section is straight and has no downhill slope. The groundwater level is about 12 m. The excavation size of the bored tunnel is 10 m (width) × 9.83 m (height). The construction method of the tunnel is shield tunneling before expansion tunneling, and the structure is composite lining.

The "cup" freezing wall is used to strengthen the soil at the beginning of the shield. The thickness of the "cup bottom" is 3.0 m, the length of the "cup wall" is 10 m, and the thickness is 1.5 m. The average temperature of the freezing wall at the bottom of the cup should not be higher than −10 °C, the average temperature of the freezing wall at the wall of the cup should not be higher than −8 °C, and the average temperature at the interface between the freezing wall and the underground continuous wall should not be higher than −5 °C. The freezing wall design is shown in Figure 2. The frozen construction situation on site is shown in Figure 3.

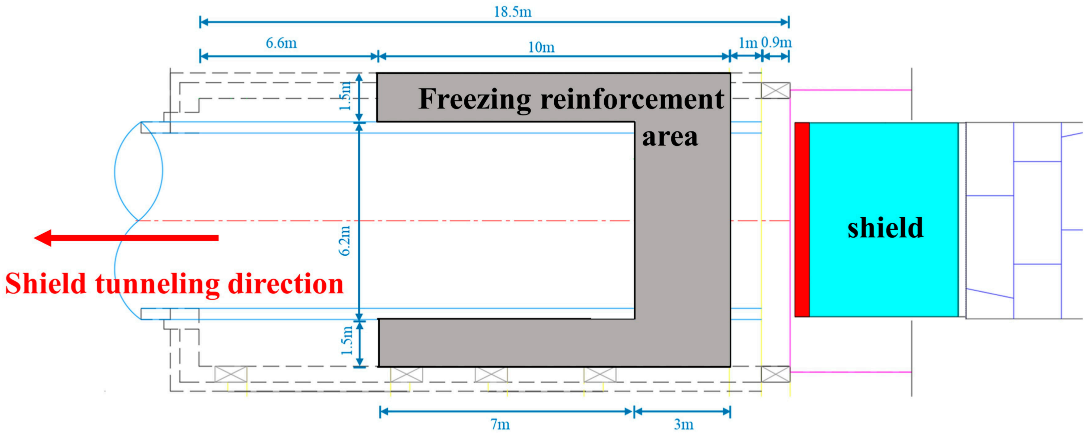

Figure 2. Freeze section plan.

Figure 3. Frozen construction drawing on site.

2.2. Geological Situation

(1) The strata are mainly composed of quaternary loose sediments, the underlying bedrock is buried deep, and the quaternary overburden thickness is larger, all of which are over 50 m.
(2) Artificial accumulation layer: the surface layer along the project is covered with artificial accumulation layer, which is mainly sandy silt fill and miscellaneous fill.
(3) Quaternary alluvium: It is distributed under the artificial accumulation layer. The lithology is mainly clay, silt, and sand layers, and the stratigraphic distribution is relatively stable.

The site situation of some soil layers is shown in Figure 4. The viscous soil layer and sandy soil on the site contain calcareous nodules, with many local areas, unstable distribution, complex contents, irregular cementation degree, etc.; with high strength, it is not easy to break, and it is located within the scope of the shield in this section, which makes it easy to wear down and destroy the cutter head during shield construction, creating adverse conditions during shield construction.

(**a**) (**b**)

Figure 4. Field soil condition: (**a**) borehole sampling of soil; (**b**) silt.

2.3. Monitoring Scheme

We investigated the buildings or structures and their surrounding conditions within the influence range of the intersectional tunnel and determined that an Industrial and Commercial Bank of China (ICBC) office and a mosque should be included in the monitoring range, as shown in Figure 5. The ICBC office building is a six-level frame structure. The horizontal distance between the shield tunnel and the ICBC office building is 3.24 m, and the vertical distance between the shield tunnel and the foundation is 18.89 m. The mosque is a four-level frame structure with a natural foundation. The horizontal distance between the shield tunnel and the mosque is 3.95 m, and the vertical distance between the shield tunnel and the foundation is 18.82 m.

(**a**) (**b**)

Figure 5. Real scene of the building: (**a**) Industrial and Commercial Bank of China; (**b**) xiaolou mosque (The Chinese character in the picture is the name of the shop).

According to the actual site conditions and the requirements of measuring point layout, 17 surface settlement monitoring points were set up. The surface settlement monitoring points were arranged along the surface above the tunnel axis, and the measuring points were labeled DBC 1-1 to DBC 1-17. Six vertical displacement monitoring points were set up at the corners of external walls, load-bearing columns, and external walls, with the measuring points numbered from JGC-1 to JGC-6. The details of the measuring point arrangement are shown in Figure 6.

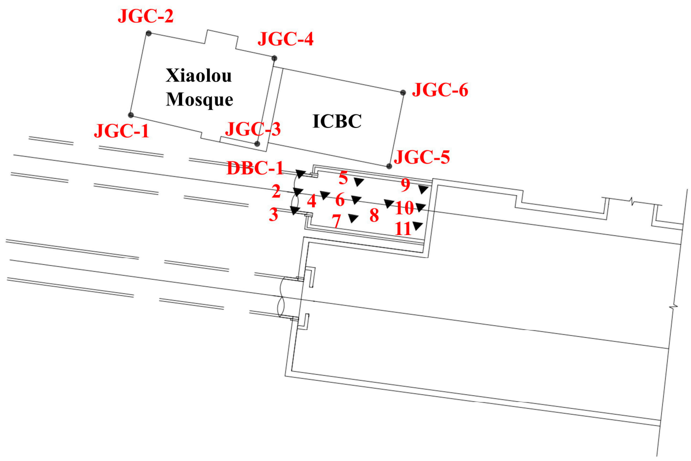

Figure 6. Layout of measuring points.

3. Numerical Model Establishment and Excavation Simulation

3.1. Geometry and Boundary Conditions

The numerical model was established using Plaxis 3D finite element software. According to the actual working conditions and software computing power, the scope of the model was selected. The X direction was -60 m $\leq X \leq 80$ m; Y direction was -79.5 m $\leq Y \leq 80$ m. The Z direction was -46 m $\leq Z \leq 15$ m. The model is shown in Figure 7. The groundwater level was set to 12 m. Triangular grids were used to divide numerical models. The metro station and building grid size was 1; the other grid sizes were 1–3. Through meshing, the model was divided into 407,364 units and 544,132 nodes. Using uniform boundary conditions, X-directional displacement constraints were imposed on the X-directional boundary of the model; Y-directional displacement constraints were imposed on the Y-directional boundary; and X-, Y-, and Z-direction displacement constraints were imposed on the bottom boundary of the model. The top boundary of the model in the Z-direction was considered a free boundary.

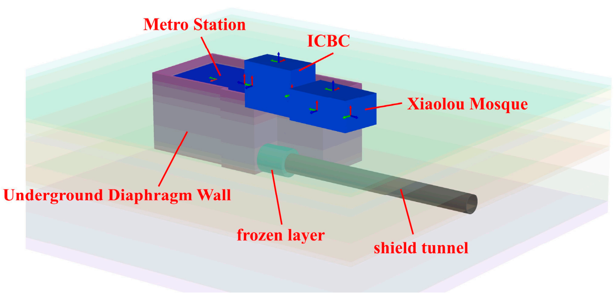

(**a**)

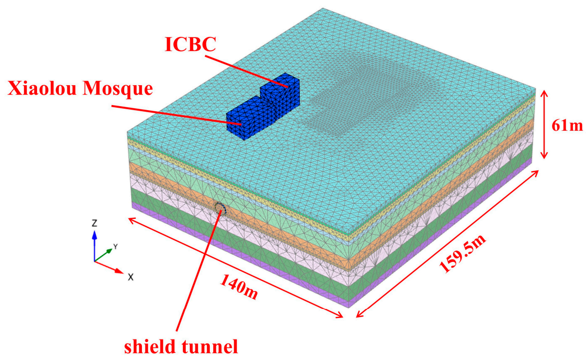

(**b**)

Figure 7. Numerical model: (**a**) model geometry; (**b**) grid division.

3.2. Material Properties

All soil layers were assumed to be elastoplastic and isotropic materials. The Mohr–Coulomb model was used to simulate soil materials. The underground diaphragm wall and shield segment were simulated by concrete structure. The upper building was simulated by plate structure. Interface units were used in Plaxis software to simulate the interaction between materials. The reduction factor of the interface element was set at 0.67. The lateral pressure of soil was calculated according to the static earth pressure. The material parameters in the numerical model were derived from geological engineering survey reports.

The mechanical indexes of material and soil are shown in Tables 1 and 2, respectively. The lining adopts a reinforced concrete structure. The inner diameter of the lining is 5.5 m and the outer diameter is 6.2 m. The thickness of the segment is 0.35 m and the width is 1.5 m.

Table 1. Material mechanics parameters.

Material	Density (kg/m^3)	Elastic Modulus (kN/m^3)	Poisson Ratio
Shield tunnel segment	2700	3.1×10^7	0.1
Floor	2500	2.21×10^7	/

Table 2. Mechanical indexes of soil layers.

Number	Stratum	Density (kg/m^3)	Elastic Modulus (MPa)	Secant Modulus (MPa)	Unloading Modulus (MPa)	Cohesive Forces (kPa)	Angle of Friction (°)	Permeability Coefficient (m/d)
1	Fill	1850	5	5	25	10	15	0.5
2	Fill of Sand	1750	5	5	25	15	18	0.5
3	Sandy silt	1910	9.2	9.2	27.6	17	23	0.5
4	Clayey silt	1990	6.3	6.3	31.5	24	16	0.05
5	Silt	2050	20	20	60	0	28	4
6	Fine sand	2070	25	25	75	0	32	5
7	Silty clay 1	2000	6.4	6.4	32	31	21	0.05
8	Silty clay 2	1960	7.2	7.2	36	34	22	0.05
9	Silty clay 3	1960	8.2	8.2	41	36	24	0.05
10	Frozen soil	2000	100	38.46	134.6	200	5	0.5

3.3. Excavation Simulation

Simulation left-line tunnel excavation 66m, a total of 44 rings. Grouting was not considered in the excavation process. Without considering the influence of the freeze–thaw cycle, only the shield excavation process was simulated. According to the site conditions, design data, and construction plan, the corresponding construction process was simulated. The specific construction stages are as follows:

(1) In the initial stage, only gravity load is applied to generate the initial stress field of the stratum.
(2) In the freezing construction, the displacement caused by each stage in the early stage is cleared. The stress field is retained and the corresponding parameters of the designed freezing zone outside the tunnel are changed to frozen soil parameters.
(3) When the shield is excavated for one ring, the surface load of the excavation face is activated to act as the earth pressure to maintain the balance of the excavation face.
(4) When the shield machine continues to excavate, the first ring segment is activated. When the shield machine is driven to the second ring, the surface load of the excavation face at the first ring is frozen. Meanwhile, the surface load of the excavation face at the second ring is activated.
(5) Cycle steps (3) and (4) until excavation to the 44th ring.

4. Effects of Freezing Excavation of Shield Tunnel on Segments, Soil Layer, and Vertical Displacement of Buildings

4.1. Deformation Analysis of Shield Segment

4.1.1. Deformation of Shield Segment in Frozen Layer

We selected the shield segment with the largest displacement during frozen layer excavation, as shown in Figure 8.

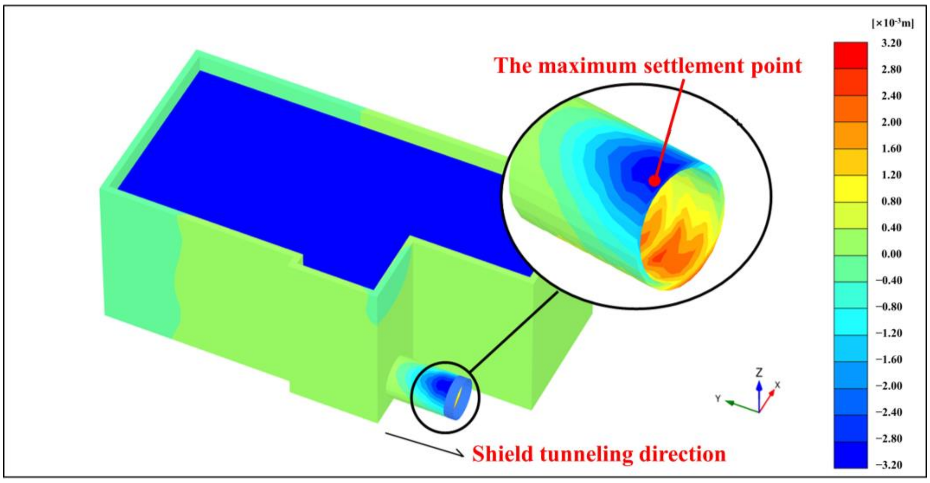

(**a**)

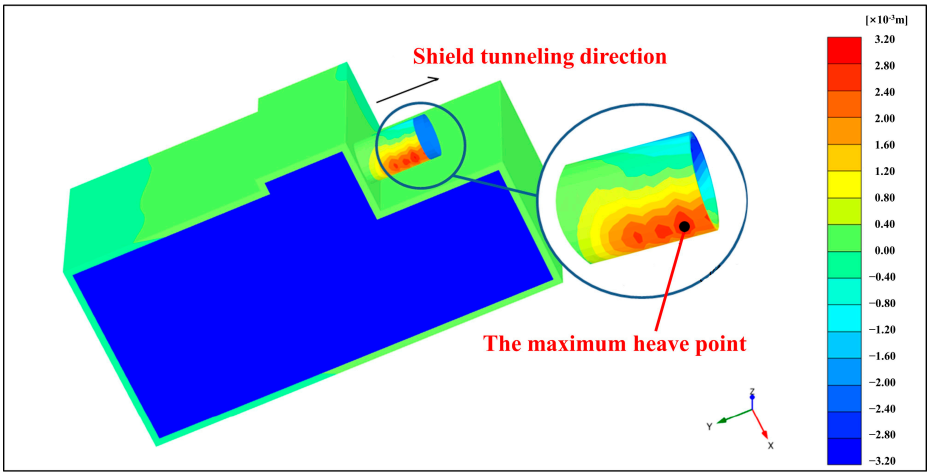

(**b**)

Figure 8. Deformation of frozen layer segment: (**a**) maximum settlement; (**b**) maximum heave.

(1) The frozen layer strengthened the elastic modulus and stability of the soil, and the soil disturbance caused by tunnel excavation was reduced accordingly. The displacement of segments in the frozen layer was analyzed using numerical simulation. The maximum settlement value of the segment caused by tunnel excavation was 3.1 mm, and the maximum settlement point was located at the crown of the segment, close to the connection between the frozen layer and the nonfrozen layer. The maximum heave value of the segment was 2.9 mm, and the maximum heave point was located at the bottom of the segment, which is also near the connection between the frozen layer and the nonfrozen layer.

(2) In general, the frozen layer plays an important role in reducing the soil disturbance caused by shield excavation. The maximum settlement and heave occurred at the junction of the frozen and nonfrozen layers because the elastic modulus and integrity of the soil in the nonfrozen layer were weakened. The maximum settlement value and the maximum heave value of the segment were used to calculate the convergence of the segment in the limit state. The convergence value of the ultimate clearance was 6 mm, which meets the control value of 12.4 mm clearance convergence required by the standard [23].

4.1.2. Deformation of Shield Segment in Nonfrozen Layer

We selected the shield segment with the largest displacement during nonfrozen layer excavation, as shown in Figure 9.

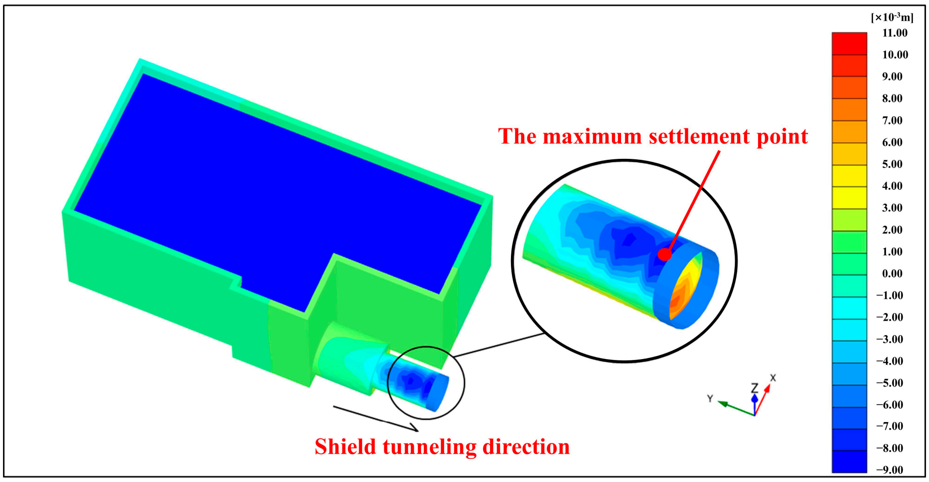

(**a**)

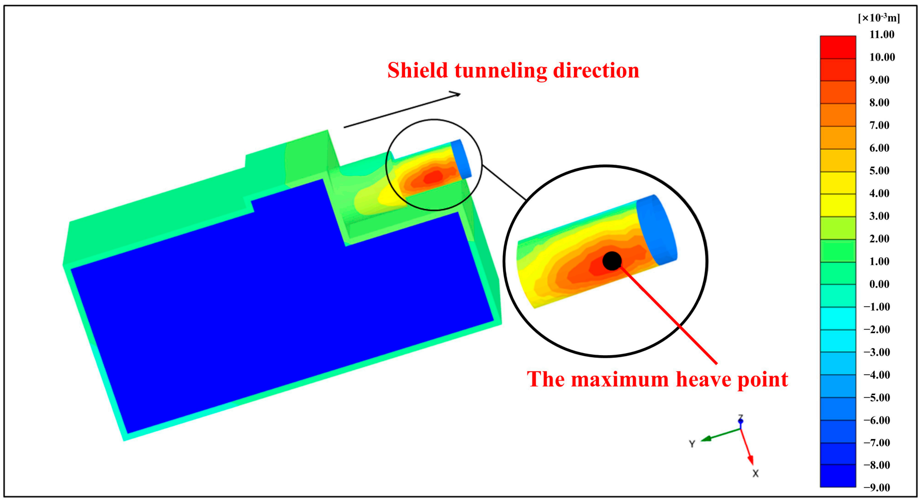

(**b**)

Figure 9. Cloud image of segment deformation during nonfrozen layer excavation: (**a**) the maximum settlement of segments during the excavation of nonfrozen layer; (**b**) the maximum heave of segments during the excavation of nonfrozen layer.

(1) When excavation is carried out in the nonfrozen layer, because of the lack of reinforcement of the frozen layer, the soil disturbance increases the displacement of the segment. The displacement of segments in the nonfrozen layer was analyzed using numerical simulation. The maximum settlement value of segment caused by tunnel excavation was 8.6 mm, and the maximum settlement point was located at the crown of segment. The maximum heave value of the segment was 10 mm, and the maximum heave point was located at the bottom of the segment.

(2) The maximum settlement value and the maximum heave value of the segment were used to calculate the convergence of the segment in the limit state. The convergence value of the ultimate clearance was 18.6 mm, which did not meet the control value of 12.4 mm clearance convergence required by the standard [23]. The main reason is that synchronous grouting was not considered in the numerical simulation, which caused the displacement of the segment to be too large.

To sum up, it can be seen that:

(1) The segment displacement caused by the shield in the frozen layer is within the reasonable range controlled by the standard [23]. The main reason for the large displacement of pipe segments caused by excavation in the nonfrozen layer is that

the effect of grouting was not considered in the numerical simulation. Supervision should be strengthened in field construction to avoid construction accidents.

(2) During excavation, the segment displacement of the frozen layer is about one-third of that of the nonfrozen layer. The frozen layer effectively improves the stability of the soil; the elastic modulus of the soil is increased by about 5–10 times. The segment displacement caused by shield tunneling is effectively reduced.

4.2. Surface Settlement Analysis

As shown in Figure 10, the surface settlement was taken as the ordinate, and the shield construction to a certain segment was taken as the abscissa. Numerical simulations and field data were linked at this point in time. Field data were measured once a day, so they are not continuous. The settlement values of the 11 measuring points on the surface were all effectively controlled at between −2 mm and 2 mm, the maximum surface heave value was 1.7 mm, and the maximum surface settlement value was 1.8 mm, both of which met the control requirements of the standard [23]. The numerical simulation results of surface settlement are consistent with the settlement law of field data. The error between the field data and the simulated data was mainly due to the fact that the soil disturbance caused by grouting and the freeze–thaw cycle was not considered in the numerical simulation. The error between the them was small, which verifies the correctness of the numerical model.

(1) The strata were uniformly arranged horizontally when the model was established, and the inclined strata were not set.
(2) The effect of grouting was not considered in the numerical simulation.
(3) The assumption that the lining is an elastic material led to differences from the field situation.

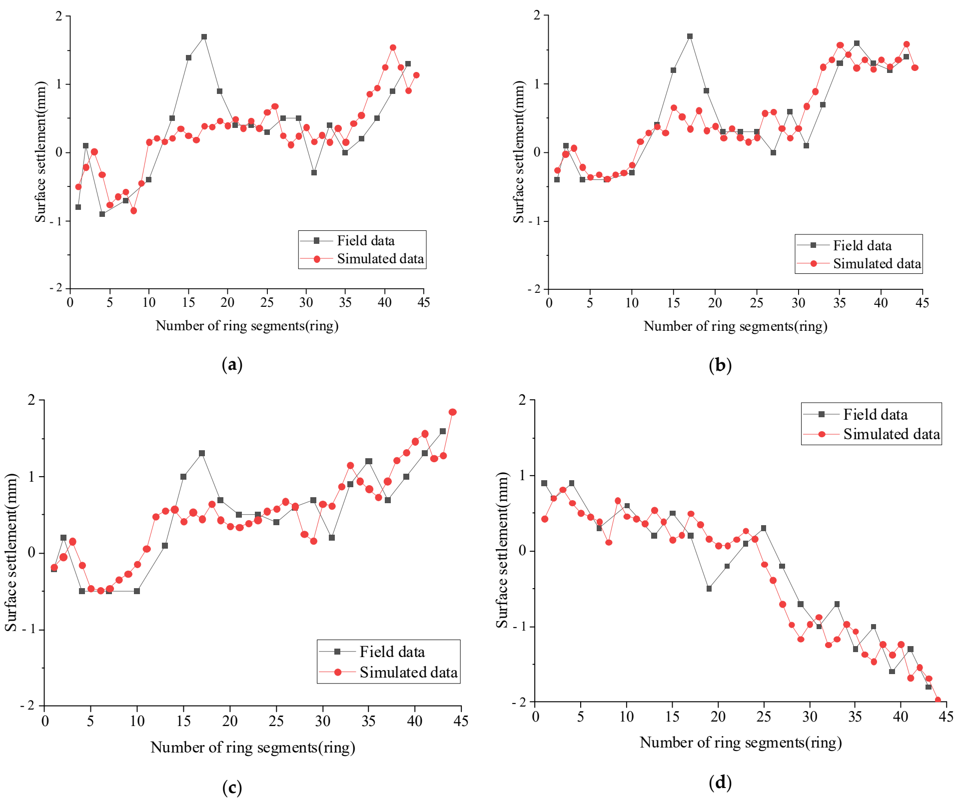

Figure 10. *Cont.*

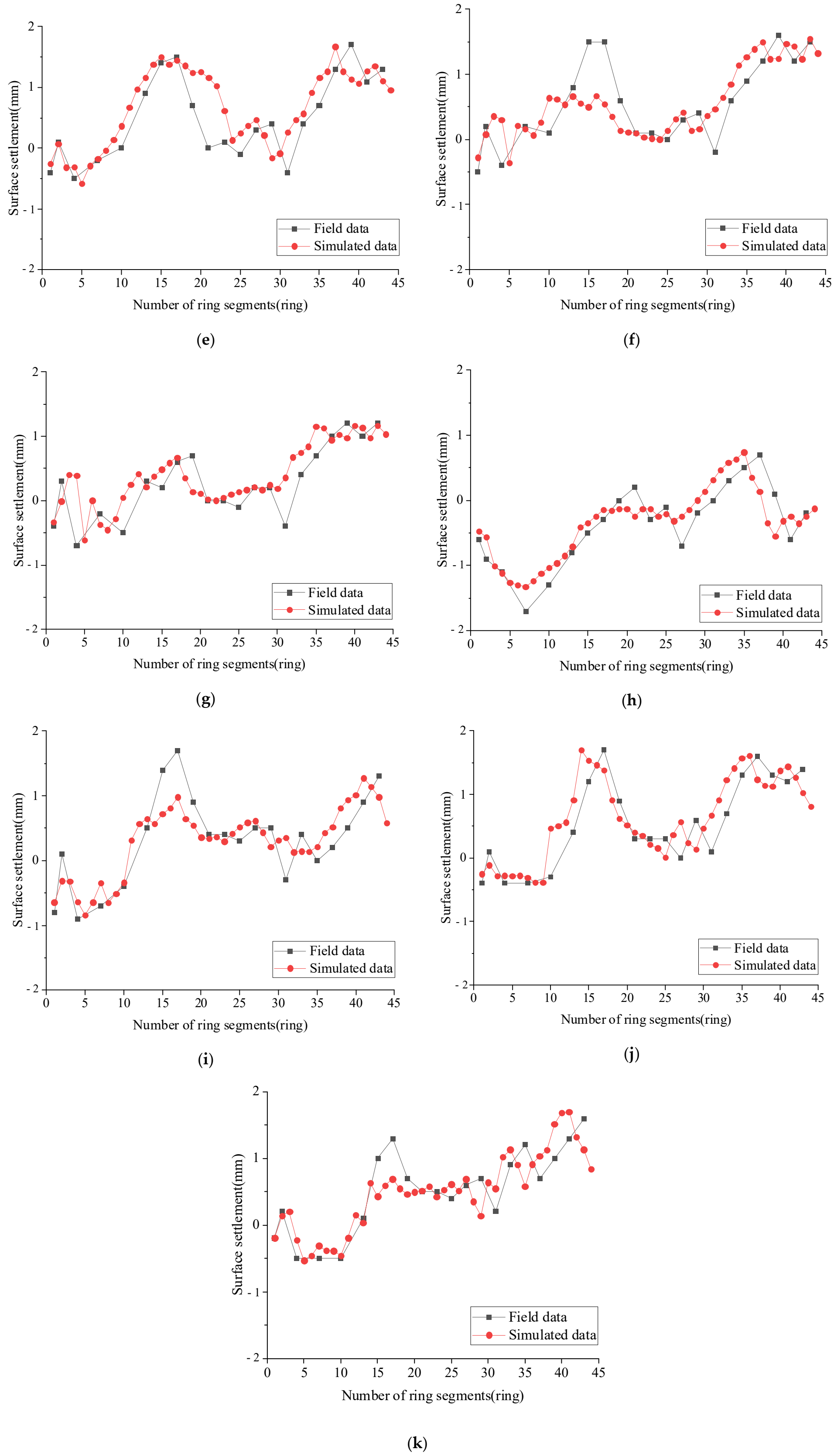

Figure 10. Surface settlement caused by freezing shield excavation: (**a**) DBC-1; (**b**) DBC-2; (**c**) DBC-3; (**d**) DBC-4; (**e**) DBC-5; (**f**) DBC-6; (**g**) DBC-7; (**h**) DBC-8; (**i**) DBC-9; (**j**) DBC-10; (**k**) DBC-11.

The following conclusions can be drawn from the data from the 11 surface-monitoring points:

(1) Except for the surface settlement data from DBC-4, the surface displacement above the frozen layer is mainly upward heave. Because of the good stability of the frozen layer, it is difficult to deform the soil downward. However, in the process of shield excavation, the face pressure leads to the overall upward deformation of the frozen layer, and finally the surface displacement becomes a state of heave.

(2) In the process of shield excavation, the soil disturbance is further reduced because the frozen layer is close to the underground diaphragm wall of the station. The surface settlement is within the allowable range of the standard [23]. The frozen layer effectively controls the surface settlement.

4.3. Vertical Displacement Analysis of Buildings

The vertical displacement of the building is shown in Figure 11, where the data of JGC-4 was lost.

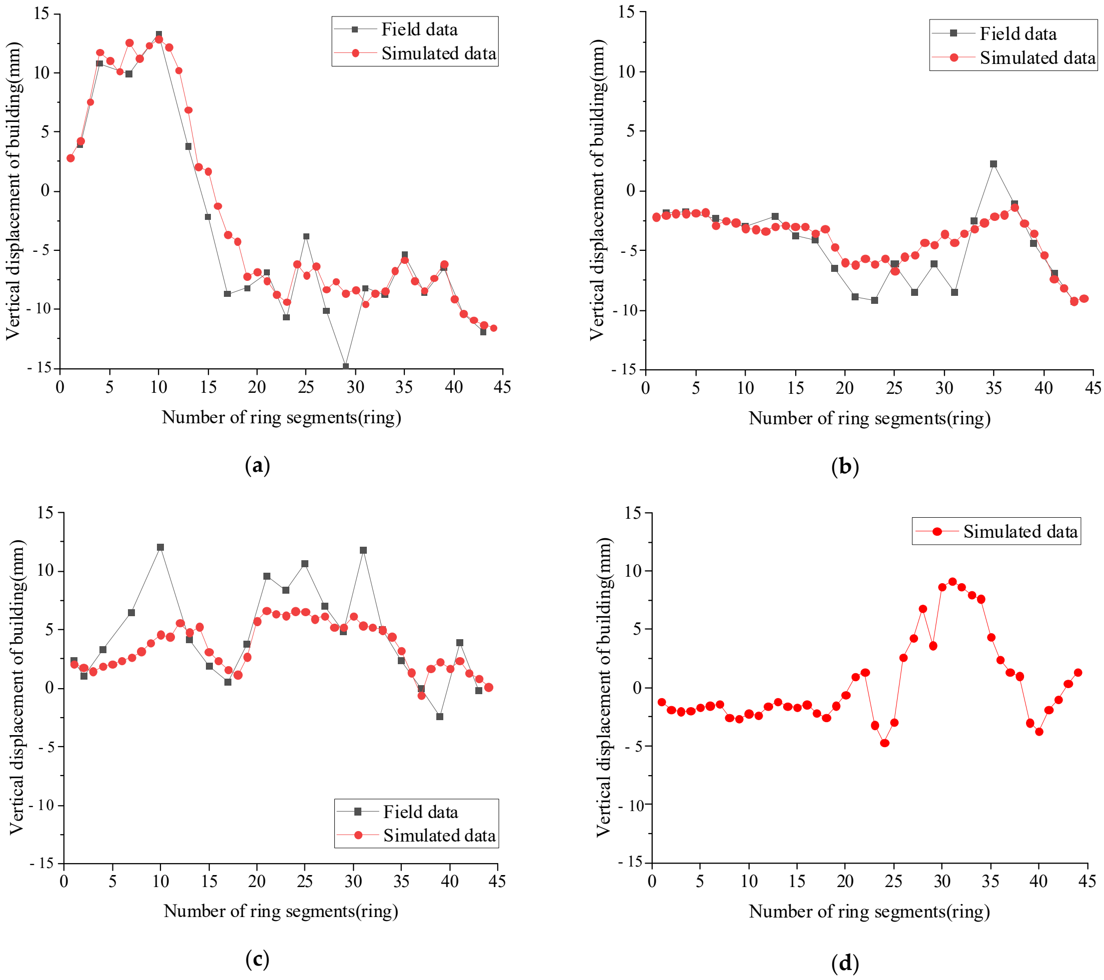

Figure 11. *Cont.*

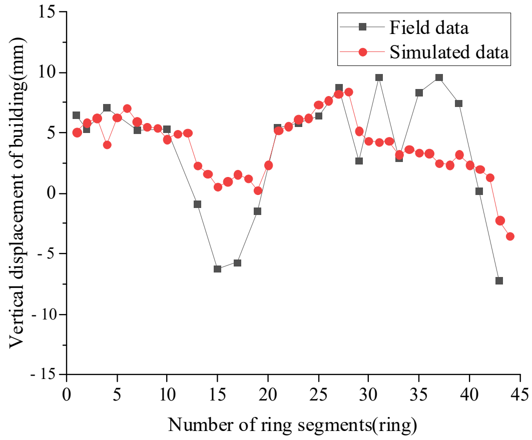

(**e**)

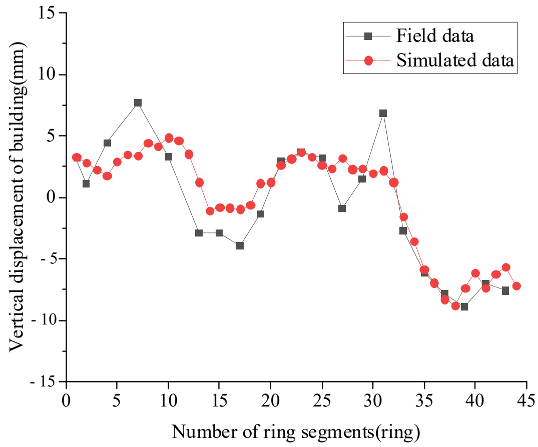

(**f**)

Figure 11. Vertical displacement of adjacent buildings under shield freezing excavation: (**a**) JGC-1; (**b**) JGC-2; (**c**) JGC-3; (**d**) JGC-4; (**e**) JGC-5; (**f**) JGC-6.

(1) JGC-1, JGC-3, and JGC-5 are vertical displacement monitoring points of buildings near the tunnel. Before the tenth step, the three monitoring points produced heave, and the heave value of JGC-1 was the largest, with a maximum of 10 mm. The main cause of the heave was the disturbance of the soil in front of the shield face pressure. After the tenth step, the settlement of JGC-1 occurred rapidly, and the maximum settlement value was 15 mm. The maximum settlement value of JGC-3 and JGC-5 did not exceed 5 mm. The main reason is that the frozen layer strengthens the soil, and the surface settlement of JGC-1 and JGC-3 near the frozen layer is also relatively small.

(2) JGC-2, JGC-4, and JGC-6 are vertical displacement monitoring points of buildings away from the tunnel. A large heave occurred at JGC-4, with a maximum heave value of 14.7 mm. The main reason was that the elastic modulus of soil at the boundary of the frozen layer and nonfrozen layer became smaller, and the soil stability became worse. At this time, JGC-4 was rapidly heaved under the influence of the shield face's pressure. The other two measuring points mainly experienced settlement displacement, and the maximum settlement value was 11.9 mm.

(3) JGC-5 and JGC-6 are in the same cross-section but at different distances from the frozen layer. The maximum settlement value of JGC-6 was 9.8 mm. The maximum settlement value of JGC-5 was 4.9 mm. JGC-5 is located above the frozen layer, which strengthens the surrounding soil and restrains the deformation of the soil. JGC-6 is far away from the frozen layer, the formation disturbance caused by excavation was obvious, and the strengthening effect of the frozen layer was weak. Finally, the settlement velocity and value of JGC-6, which is far away from the frozen layer, were greater than that of JGC-5.

(4) The maximum vertical settlement difference between JGC-1 and JGC-2 was 14.8 mm. The maximum vertical settlement difference between JGC-3 and JGC-4 points was 14.1 mm. The maximum vertical settlement difference between JGC-5 and JGC-6 points was 13.9 mm. These data were less than 15 mm, within the range required by the standard [23]. The differential settlement of the buildings meets the requirements.

To sum up, the building displacement on the boundary of the frozen layer and non-frozen layer should be strictly monitored during construction to avoid large displacement and deformation in the area where soil properties change. At the same time, the settlement of buildings far away from the same cross-section of the frozen layer should be strictly monitored. The disturbance caused by the excavation in this area is also relatively large, and the strengthening effect of the frozen layer weakens faster.

5. The Influence of Frozen Layer, Soil, and Vertical Displacement of Building Caused by Frozen Expansion of Shield Tunnel

5.1. Support Design Parameters

This project adopted AFM reinforcement and mining expansion construction. The primary lining was made of C25 shotcrete and steel grid frames with a spacing of 0.5 m. The secondary lining was made of C35 molded concrete with a waterproof grade of P10.

The construction scheme of the underground station tunnel with main structure was freezing first and then expanding. The construction step comprised freezing the soil outside the underground station tunnel first to form a high-strength and well-sealing permafrost curtain. Then, the existing tunnel was constructed using the mining method in the frozen layer.

The length of the frozen layer was 22.5 m The diameter of the freezing tube and pressure relief tube was 108 mm and the thickness was 8 mm. The diameter of the horizontal temperature measuring tube was 89 mm and the thickness was 8 mm. The diameter of the inclined temperature measuring tube was 45 mm and the thickness was 4.5 mm. The diameter of the liquid supply pipe was 45 mm and the thickness was 4.5 mm. The pipe was made of no. 20 high-quality carbon steel. The frozen pipe used a threaded connection or a weld connection, and its connection strength was not less than 75% of the strength of the rigid pipe.

The effective thickness of the outer frozen wall was 3.0 m. The average temperature of the freezing wall was not higher than −10 °C. The frozen layer design of the excavation section is shown in Figure 12.

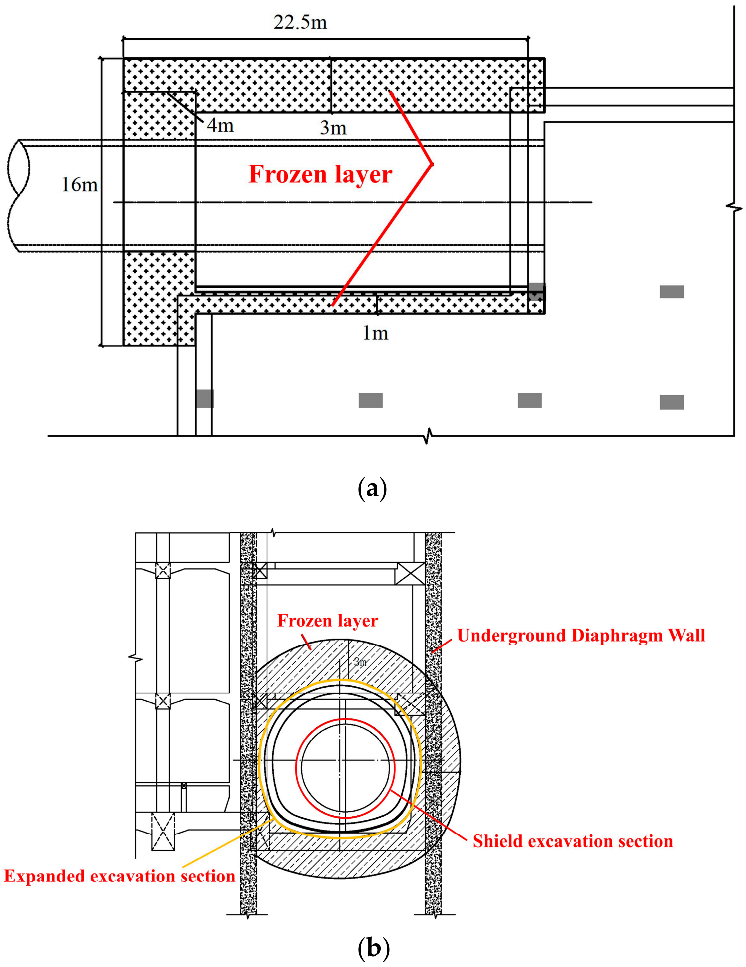

Figure 12. Freezing layer design: (**a**) top view of the frozen layer; (**b**) frozen layer profile.

5.2. Tunnel Freezing Expansion Simulation

C25 shotcrete and grille steel frames were used as primary lining with a thickness of 0.3 m. C35 reinforced concrete was used as a secondary lining with a thickness of 0.5 m and a waterproof rating of P10. The primary lining was used to convert the elastic modulus of the steel grille steel frame to the shotcrete. The material parameters of the primary lining and secondary lining are shown in Table 3.

Table 3. Mechanical parameters of materials.

Materials	Density (kg/m^3)	Elastic Modulus (kN/m^3)	Poisson's Ratio
Primary lining	2500	3.08×10^7	0.2
Secondary lining	2500	3.15×10^7	0.2

The specific steps of the two construction methods are as follows:

(1) The full-face frozen excavation method

The full-face frozen excavation method was adopted to expand the excavation; each time, the whole section was excavated 1.5 m, and the primary lining and secondary lining were applied after the excavation was completed, totaling 12 steps.

(2) The partial face frozen excavation method

This four-step excavation method was adopted for partial excavation. Each excavation was 1.5m, and the specific excavation steps of each ring are shown in Figure 13. There are 29 excavation steps, as follows:

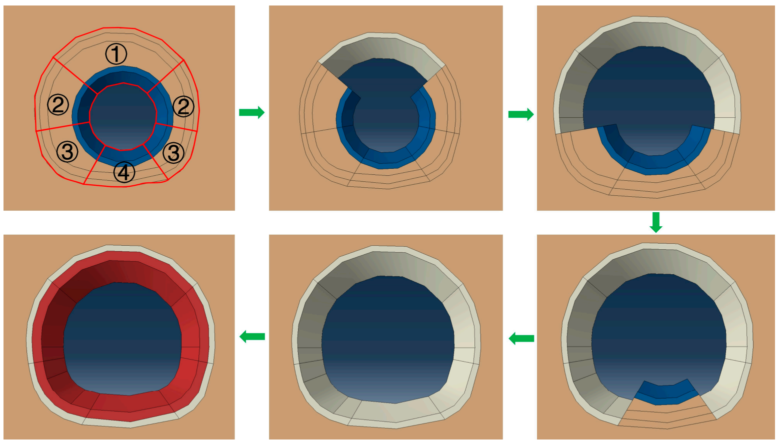

Figure 13. Schematic diagram of sectional excavation.

Steps 1–4: Excavate the first ring (1), (2), (3), and (4).
Step 5: Add the secondary lining of the first ring and excavate the second ring (1).
Step 6: Excavate the second ring (2).
Step 7: Excavate the second ring (3) and third ring (1).
Step 8: Excavate the second ring (4) and third ring (2).
Step 9: Add the secondary lining of the second ring, excavate the third ring (3), and excavate the fourth ring (1).
. . . . . .
Step 29: Add the secondary lining of the 12th ring.

5.3. Frozen Expansion Results of Shield Tunnel

5.3.1. The Full-Face Frozen Excavation Method

The numerical simulation results of full-face frozen excavation are shown in Figure 14. During the excavation simulation, the maximum value of frozen layer deformation was

45.43 mm. The whole frozen layer area had a large deformation, and even some soil collapse, so it would be impossible to adopt the full face excavation method.

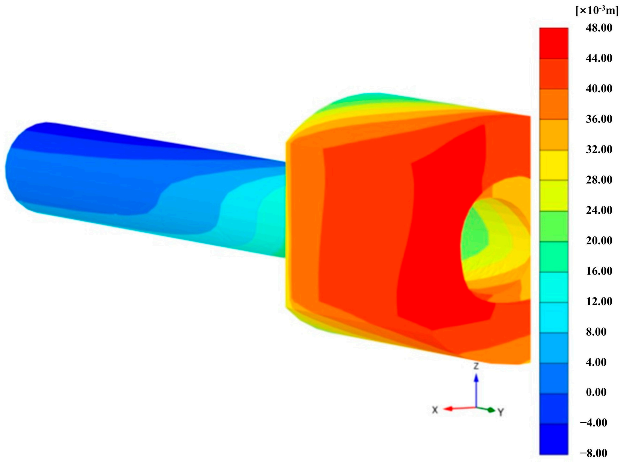

Figure 14. Deformation of frozen layer in full-face excavation.

5.3.2. The Partial Face Frozen Excavation Method

(1) Deformation analysis of frozen layer

The deformation of the frozen layer caused by partial face frozen excavation is shown in Figure 15. The maximum settlement value was 3.1 mm, and the maximum settlement point was located at the tunnel base. The maximum heave value was 10 mm, and the maximum heave point was located at the tunnel roof. The deformation of the frozen layer caused by the partial face excavation meets the requirements of the standard [23]. The deformation of frozen layer was smaller than the influence caused by the full-face excavation, so the partial face frozen excavation method should be used to expand excavation.

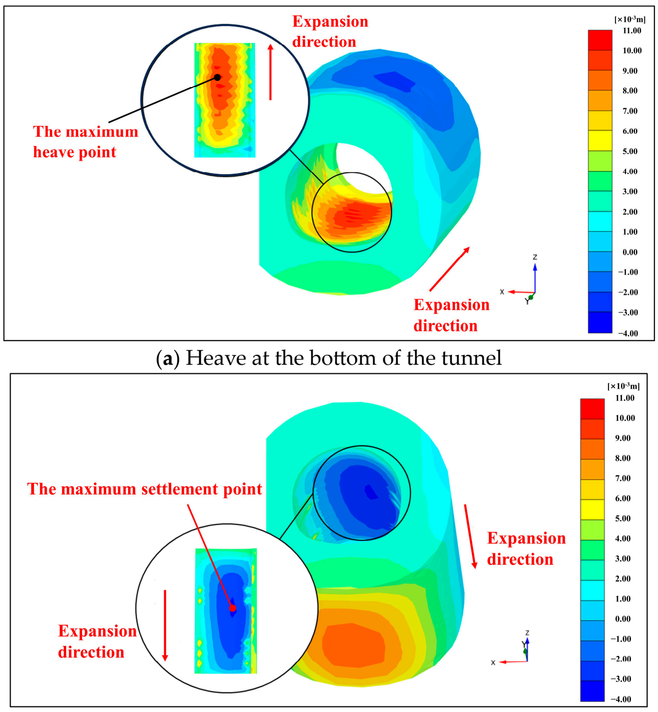

(**a**) Heave at the bottom of the tunnel

(**b**) Tunnel roof settlement

Figure 15. Frozen layer deformation caused by partial face frozen excavation: (**a**) heave at the bottom of the tunnel; (**b**) tunnel roof settlement.

(2) Analysis of land surface settlement

The numerical simulation results of surface settlement are shown in Figure 16. The following conclusions were drawn:

(1) DBC-9 to DBC-11 is located directly above the initial expansion part. Surface settlement occurred at the beginning of excavation, the surface settlement gradually increased to 2.5 mm, and then the soil disturbance gradually stabilized. As the frozen layer strengthened the soil, the surface settlement did not increase.

(2) DBC-4 to DBC-8 is directly above the middle of the expansion section. At the beginning of excavation, surface heave occurred, and the surface heave value gradually increased to 1.6 mm. With the progress of excavation, the disturbance of excavation to soil gradually increased, and the surface displacement gradually changed from heave to settlement. When the surface settlement value reached 2.5 mm, the surface settlement tended to be stable and no longer increased.

(3) DBC-1 to DBC-3 is at the end of the expansion section. At the beginning of excavation, the monitoring point was relatively far away from the excavation tunnel. The surface displacement was mainly heave, and the maximum heave value was less than 1 mm. The three monitoring points are located at the boundary between the frozen and non-frozen layers. With the progress of excavation, the disturbance of soil increased. The surface displacement gradually changed from heave to settlement, and the maximum settlement value reached 2.7 mm. There was no stable trend of surface settlement.

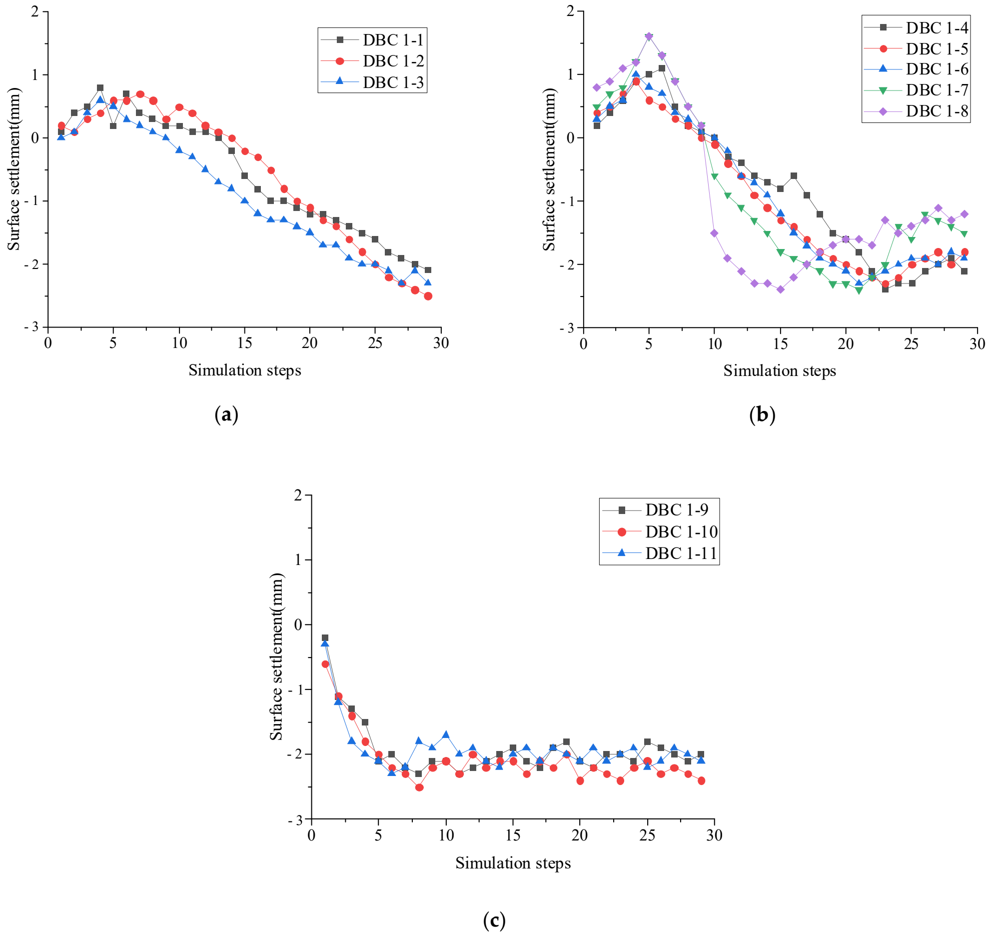

Figure 16. Surface settlement caused by partial face frozen excavation: (**a**) DBC-1 to DBC-3; (**b**) DBC-4 to DBC-8; (**c**) DBC-9 to DBC-11.

In summary, the frozen layer can improve the stability of soil in the process of construction. The underground diaphragm wall also has a good reinforcement effect on the surrounding soil. The stratum disturbance caused by excavation under the combined action of the two is well controlled. The surface settlement is controlled within the allowable range of the standard [23].

(3) Vertical displacement of buildings

The numerical simulation results of vertical displacement of buildings are shown in Figure 17. The following conclusions can be drawn:

(1) JGC-1, JGC-3, and JGC-5 are vertical displacement monitoring points of buildings near the tunnel. JGC-5 is closest to the expanded tunnel, and the soil disturbance is the most intense. The settlement of JGC-5 was severe in the whole process of expansion. The maximum settlement value was 8.3 mm and then tended to be stable. The settlement trends of JGC-3 and JGC-1 were basically the same, and the maximum settlement value was 6.2 mm. The settlement displacements of the three monitoring points were all within the allowable range of the standard [23], which proves the practicability of the partial face frozen excavation method.
(2) JGC-2, JGC-4, and JGC-6 are the vertical displacement monitoring points of buildings away from the tunnel. JGC-6 rapidly settled with a maximum settlement value of 8.1 mm. JGC-2 and JGC-4 were heaves with maximum bulges of 4 mm.
(3) JGC-5 and JGC-6 are in the same cross-section of the frozen layer but at different distances. Before step 10, JGC-6 settled relatively quickly. The maximum settlement value was 4.1 mm. Before step 10, JGC-5 settled slowly. The maximum settlement value was 2.2 mm. The main reason is that JGC-5 is close to the frozen layer, which strengthens the surrounding soil and restrains the deformation of the soil. Although JGC-6 is farther away than JGC-5, the hardening effect of the frozen layer is weaker, and the soil disturbance is more obvious.
(4) Among the six measuring points, the largest building settlement difference was 12.3 mm. These data were less than 15 mm, within the range required by the standard [23]. The differential settlement of the buildings meets the requirements.

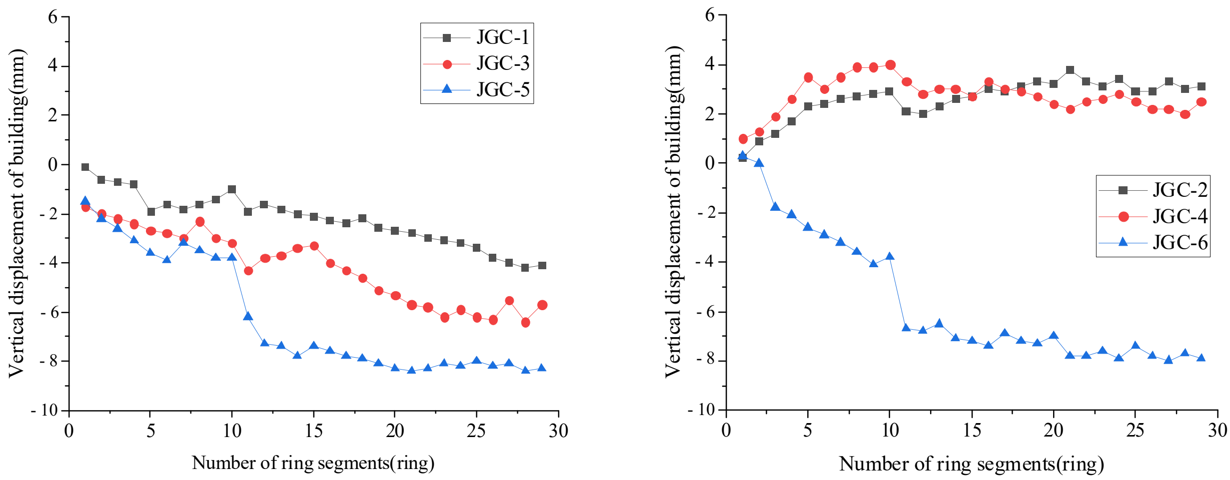

(**a**) (**b**)

Figure 17. Vertical displacement of building caused by partial face frozen excavation: (**a**) JGC-1, JGC-3, and JGC-5; (**b**) JGC-2, JGC-4, and JGC-6.

In summary, the settlement of buildings was within the allowable range of the standard [23], which proves the practicability of excavation. During construction, it is necessary to strengthen monitoring of the settlement of buildings far away from the same cross-section of the frozen layer to avoid construction accidents caused by excessive settlement.

5.4. Construction Safety Control Measures

In order to reduce frozen soil deformation and ground settlement, the following measures should be adopted in site construction:

(1) In the process of excavation, temporary steel supports should be set in time. Horizontal and vertical reinforcement supports should be set.
(2) Grouting behind the freezing wall should be performed in time after excavation.
(3) The top of the frozen soil should be set up with pressure relief holes. According to the monitoring of surface settlement, grout should be injected during settlement and released during heave.
(4) Real-time dynamic monitoring of the temperature of the frozen pipe and the melting of frozen soil should be implemented, and emergency plans should be made.

6. Recommendations and Limitations

For similar water-rich sand layer subway station projects, the following suggestions can be referred to:

(1) Surface settlement or vertical displacement of buildings at the boundary between frozen and nonfrozen layers should be strictly monitored.
(2) The surface settlement or vertical displacement of buildings far away from the same cross-section of the frozen layer should be strictly monitored.
(3) For the expansion of large diameter shield tunnel, the partial face excavation method should be preferred.

The limitations of this study are as follows:

(1) This study is for water-rich sand strata, and the conclusions drawn may not be applicable to rock strata.
(2) In the numerical simulation, the lining and shield are regarded as linear elastic materials, and the soil is regarded as a uniform elastic–plastic material. These assumptions lead to some errors between the numerical model and the actual project.
(3) The numerical simulation does not consider the influence of grouting and the freeze–thaw cycle. It can be added to the numerical simulation in future research to further improve the accuracy of the numerical model.

7. Conclusions

This paper relied on a water-rich sand clay formation freezing method to construct a metro station project. According to the construction sequence of frozen layer shield excavation to frozen layer expansion excavation, the deformation of segment, frozen layer, surface settlement, and vertical displacement of a building caused by construction were studied. The main conclusions are as follows:

(1) The deformation of the lining in the nonfrozen layer is about three times that of the lining in the frozen layer. The convergence of the ultimate clearance of the lining in the nonfrozen layer is 1.5 times that of the lining in the frozen layer. The maximum deformation value of the frozen layer in full section excavation scheme is 4.5 times that of the frozen layer in partial excavation. Through these data, it can be found that the freezing layer has an obvious effect on limiting the displacement of the lining.
(2) When the tunnel is excavated normally, the surface settlement value above the frozen layer is within 2 mm. The surface settlement values above the frozen layer are all within 3 mm when the subdivision is extended. The frozen layer improves the integrity and mechanical parameters of the soil, and with the reinforcement of the underground diaphragm wall, the surface settlement is effectively reduced.
(3) The vertical settlement of the building on the side away from the frozen layer is greater than that on the side near the frozen layer. The main reason is that the frozen layer strengthens the surrounding soil, but this strengthening effect decreases with increasing distance. In the numerical simulation of partial face frozen excavation, the maximum vertical settlement value of the building was 9.8 mm, and the difference

value of the maximum vertical settlement was 12.3 mm. All these data prove that the excavation is feasible.

Author Contributions: Conceptualization, X.G. and H.F.; Data curation, W.F. and S.L.; Methodology, X.G., H.F. and W.F.; Resources, S.L.; Software, X.J., J.L. and S.X.; Validation, R.W.; Visualization, H.F., W.F. and S.X.; Writing—original draft, R.W. and X.J.; Writing—review and editing, X.G. and R.W. All authors have read and agreed to the published version of the manuscript.

Funding: This research was funded by the Service Safety and Intelligent Maintenance of Rail Transit Operation Tunnels (Project No. 2022JBXT007), the General Program of National Natural Science Foundation of China (51978356), the Youth Program of National Natural Science Foundation of China (52108371), the General Program of Shandong Natural Science Foundation of China (ZR2022ME043), and the General Program of Qingdao Science and Technology Bureau of China (23-2-8-cspz-13-nsh).

Institutional Review Board Statement: Not applicable.

Informed Consent Statement: Not applicable.

Data Availability Statement: The data used to support the findings of this study are included within this article.

Conflicts of Interest: The authors declare no conflict of interest.

References

1. Jones, J.S. State-of-the-art report—Engineering practice in artificial ground freezing. *Eng. Geol.* **1981**, *18*, 313–326. [CrossRef]
2. Afshani, A.; Akagi, H. Artificial ground freezing application in shield tunneling. *Jpn. Geotech. Soc. Spec. Publ.* **2015**, *3*, 71–75. [CrossRef]
3. Russo, G.; Corbo, A.; Cavuoto, F.; Autuori, S. Artificial ground freezing to excavate a tunnel in sandy soil. measurements and back analysis. *Tunn. Undergr. Space Technol.* **2015**, *50*, 226–238. [CrossRef]
4. Li, S.; Lai, Y.; Zhang, M.; Zhang, S. Minimum ground pre-freezing time before excavation of guangzhou subway tunnel. *Cold Reg. Sci. Technol.* **2006**, *46*, 181–191. [CrossRef]
5. Han, L.; Ye, G.L.; Li, Y.H.; Xia, X.H.; Wang, J.H. In-situ monitoring of frost heave pressure during cross passage construction using ground freezing method. *Can. Geotech. J.* **2016**, *53*, 530–539. [CrossRef]
6. Zhou, J.; Zhao, W.; Tang, Y. Practical prediction method on frost heave of soft clay in artificial ground freezing with field experiment. *Tunn. Undergr. Space Technol.* **2021**, *107*, 103647. [CrossRef]
7. Liu, J.; Ma, B.; Cheng, Y. Design of the Gongbei tunnel using a very large cross-section pipe-roof and soil freezing method. *Tunn. Undergr. Space Technol.* **2018**, *72*, 28–40. [CrossRef]
8. Zhang, D.M.; Chen, C.C.; Zhang, D.M. Ground surface movement of Shallow-Buried Large-Sectional tunnel under Full-Ring Pipe-Jacking roof and ground freezing. *Tunn. Undergr. Space Technol.* **2022**, *127*, 104600. [CrossRef]
9. Cai, H.; Hong, R.; Xu, L. Frost heave and thawing settlement of the ground after using a freeze-sealing pipe-roof method in the construction of the Gongbei Tunnel. *Tunn. Undergr. Space Technol.* **2022**, *125*, 104503. [CrossRef]
10. Ding, Z.; Wei, X.J.; Wei, G. Prediction methods on tunnel-excavation induced surface settlement around adjacent building. *Geomech. Eng.* **2017**, *12*, 185–195. [CrossRef]
11. Zheng, L.; Gao, Y.; Zhou, Y. A practical method for predicting ground surface deformation induced by the artificial ground freezing method. *Comput. Geotech.* **2021**, *130*, 103925. [CrossRef]
12. Xiang, H.; Zhang, G.; Cheng, P. Analyses of the Ground Surface Displacement under Reinforcement Construction in the Shield Tunnel End Using the Artificial Ground Freezing Method. *Appl. Sci.* **2023**, *13*, 8508. [CrossRef]
13. Ren, J.; Wang, Y.; Wang, T. Numerical Analysis of the Effect of Groundwater Seepage on the Active Freezing and Forced Thawing Temperature Fields of a New Tube–Screen Freezing Method. *Sustainability* **2023**, *15*, 9367. [CrossRef]
14. Zhu, C. Surface Settlement Analysis Induced by Shield Tunneling Construction in the Loess Region. *Adv. Mater. Sci. Eng.* **2021**, *2021*, 5573372. [CrossRef]
15. Fang, Q.; Zhang, D.; Wong, L.N.Y. Shallow tunnelling method (STM) for subway station construction in soft ground. *Tunn. Undergr. Space Technol.* **2012**, *29*, 10–30. [CrossRef]
16. Bai, Q.; Zhang, Y.; Zhao, W. Construction of subway station using the small pipe roof-beam method: A case study of Shifu Road station in Shenyang. *Tunn. Undergr. Space Technol.* **2023**, *135*, 105000. [CrossRef]
17. Wang, B.; Li, Z.P.; Wang, T.; Zheng, H. A study of key construction technology on metro station constructed by enlarging large diameter shield tunnel. *Chin. Civ. Eng. J.* **2015**, *48* (Suppl. S1), 373–377.
18. Xu, X.; Li, Z.; Fang, Q. Challenges and countermeasures for using pile-beam-arch approach to enlarge large-diameter shield tunnel to subway station. *Tunn. Undergr. Space Technol.* **2020**, *98*, 103326. [CrossRef]
19. Liu, J.; Qi, T.; Wu, Z. Analysis of ground movement due to metro station driven with enlarging shield tunnels under building and its parameter sensitivity analysis. *Tunn. Undergr. Space Technol.* **2012**, *28*, 287–296. [CrossRef]

20. Li, Z.P.; Wang, T.; Zheng, H. Controlling measurements for metro station construction on enlarging large diameter shield tunnel. *Chin. J. Rock Mech. Eng.* **2015**, *34*, 1869–1876.
21. Li, X.W.; Zheng, H.; Wang, Q.H. Safety analysis for metro station constructed by enlarging large diameter shield tunnel with mining method. *Chin. Civ. Eng. J.* **2016**, *49*, 96–102.
22. Lv, J.B.; Li, X.L.; Fu, H.L.; Tang, Y.; Li, Z.R.; Zhao, H. Influence of Shield Tunnel Construction on Ground Surface Settlement under the Condition of Upper-Soft and Lower-Hard Composite Strata. *J. Vibroeng.* **2021**, *22*, 1126–1144. [CrossRef]
23. *GB 50911-2013*; Code for Monitoring Measurement of Urban Rail Transit Engineering. National Standard of the People's Republic of China: Beijing, China, 2014.